

## Condensation Heat Transfer of R22, R407C, and R410A in Slit Fin-and-Tube Heat Exchanger

Chang-Duk Jeon<sup>†</sup>, Jinho Lee\*

*Department of Mechanical Engineering, ChungJu University, ChungBuk 380-702, Korea*

*\*Department of Mechanical Engineering, Yonsei University, Seoul 120-749, Korea*

**Key words:** Alternative refrigerant, Condensation, Heat transfer coefficient, Pressure drop, R22, R407C, R410A

**ABSTRACT:** R410A and R407C are considered to be alternative refrigerants of R22 for the air-conditioners. An experimental study is carried out to investigate the effect of the change of mass flow rate on the characteristics of heat transfer and pressure drop in three row slit finned-tube heat exchanger for R407C, R410A and R22. R407C, a non-azeotropic refrigerant mixture, exhibited a quite different condensation phenomenon from those of R22 and R410A and its condensation heat transfer coefficient was much lower than that of R22 and R410A. On the other hand, the condensation heat transfer coefficient of R410A, near-azeotropic refrigerant mixture, was a little higher than that of R22. R410A also showed the lowest condensation pressure drop across the test section. For all refrigerants, the condensation heat transfer coefficient and pressure drop increase as the mass flux increases. The condensation heat transfer coefficient correlation proposed by Kedzierski shows the best agreement with the experimental data within  $\pm 20\%$ .

### Nomenclature

$A$  : area [ $m^2$ ]  
 $C_p$  : specific heat [ $kJ/kg \cdot K$ ]  
 $D$  : diameter [ $m$ ]  
 $G$  : mass flux [ $kg/m^2 \cdot s$ ]  
 $H$  : height [ $m$ ]  
 $h$  : specific enthalpy [ $kJ/kg$ ]  
 $h_{fg}$  : latent heat of vaporization [ $kJ/kg$ ]  
 $h_r$  : heat transfer coefficient [ $kW/m^2K$ ]  
 $k$  : thermal conductivity [ $W/mK$ ]  
 $L$  : length [ $m$ ]  
 $m$  : mass flow rate [ $kg/s$ ]

$P$  : pressure [ $kPa$ ]  
 $Q$  : heat transfer rate [ $kW$ ]  
 $T$  : temperature [ $^{\circ}C$ ]  
 $t$  : thickness [ $m$ ]  
 $V$  : velocity [ $m/s$ ]

### Greek symbols

$\rho$  : density [ $kg/m^3$ ]

### Subscripts

$a$  : air  
 $c$  : condensation  
 $cal$  : calculation  
 $exp$  : experiment  
 $i$  : inlet, inside  
 $l$  : liquid

<sup>†</sup> Corresponding author

Tel.: +82-43-841-5134; fax: +82-43-841-5120

E-mail address: cdjeon@chungju.ac.kr

*m* : mean  
*o* : outlet, outside  
*r* : refrigerant  
*sat* : saturation  
*sub* : subcooled  
*sup* : superheated  
*tp* : two-phase  
*v* : vapor  
*w* : wall

## 1. Introduction

R22 has been generally accepted as the most suitable refrigerant for air conditioners. However, in 1974, Rowland and Molina<sup>(1)</sup> published a paper linking CFCs with the destruction of ozone in the outer atmosphere around the earth. In the late 1980s and early 1990s governments have initiated aggressive campaigns to phase-out these compounds. The most recent revision of the Montreal Protocol at the Copenhagen conference concluded that R22 will be phased out early this century. As a result, the search for a potential replacement for R22 has been intensified in recent years.

Some of proposed potential alternatives for R22 are R407C and R410A. R407C is a zeotropic mixture consisting of 23 wt% of R32, 25 wt% of R125, and 52 wt% of R134a. R410A is an azeotropic mixture with 50 wt% of R32, and 50 wt% of R134a.

Evaporation pressure and specific compressor displacement for R407C are almost equivalent to those for R22. Therefore, it may be possible to retrofit R22 compressors with R407C if compressor displacement is taken into consideration. But system leaks may result in composition changes making service and repair more difficult. The evaporation pressure of R410A is approximately 60% higher than that of R22, the use of R410A means entirely new compressor and heat exchangers capable of withstanding higher pressure than being currently encoun-

Table 1 Comparison of physical properties of R407C and R410A

Name		R407C	R410A
Composition (wt%)	R134a	52	—
	R125	25	50
	R32	23	50
Critical temperature (°C)		86.74	72.13
Critical pressure (kPa)		4619.1	4926.1
Critical density (kg/m <sup>3</sup> )		527.3	488.9
Boiling point (°C)		-43.56	-51.53
Temperature glide		7.2	0.1
GWP (CO <sub>2</sub> =1)		1526	1725
ODP (R11=1)		0	0
$P_{sat}$ at 50°C (kPa)		2210/1985	3061/3053

tered with R22. The refrigerant properties are presented in Table 1.

A lot of studies have been reported in the literature on heat exchangers using alternative refrigerants to R22. Kim et al.<sup>(2)</sup> presented test results of a window type residential air-conditioner using R22 and two potential alternative refrigerants, R407C and R410B. For R407C, cooling capacity and efficiency were improved respectively, 2.3% and 4.1% by means of changing evaporator of a cross-parallel flow type to cross-counter flow type.

Ebisu and Torikoshi<sup>(3)</sup> performed heat transfer experiments to investigate evaporation and condensation characteristics for several alternative refrigerants flowing inside a horizontal tube, they showed that R407C introduced some complications for air-conditioning units, because it had the severe problem of heat transfer degradation during phase change, attributed to the mass transfer resistance of the zeotropic characteristics. Their results demonstrated that the average evaporation and condensation heat transfer coefficients fell about 40% and 50%, respectively, below those for R22. Ebisu and Torikoshi<sup>(4)</sup> conducted an experimental study concerning the air-cooled heat exchanger performance using R407C to clarify the effect of

the heat transfer degradation on air-cooled heat exchanger performance. Their results showed that the heat exchanger performance for R407C was about 5 to 10% lower than that for R22 in both cooling and heating modes, due to the degradation of the heat transfer coefficients of R407C.

Chen et al.<sup>(5)</sup> investigated the feasibility of using hydrocarbon refrigerant mixtures in residential air-conditioning and heat pump. AREP<sup>(6)</sup> presented results from soft-optimized system tests of several R22 alternatives and compared them with the performance of the unmodified system, run with R22. Several units were tested with R407C and R32/R125/R134a (30/10/60 by wt%) mixture. The air conditioner showed 5% decrease in cooling capacity and 2% loss in efficiency when tested with R410A.

Ryuzaburo et al.<sup>(7)</sup> tested R407C in an air-cooled packaged air conditioner and R410A in a split type room air conditioner. The volumetric capacity of R407C was found to be almost equivalent to that of R22. According to the compressor evaluation results, efficiencies of both R407C and R410A were found to be close to those of R22 within  $\pm 1\%$ .

It is an objective of the present study to investigate the effect of the change of mass flow rate on the characteristics of heat transfer and pressure drop in three row slit finned-tube heat exchanger for R407C, R410A and R22.

## 2. Experiment

### 2.1 Experimental apparatus

Figure 1 shows a schematic diagram of the present experimental apparatus. The experimental facility consists of two loops: the air loop and refrigerant loop. The wind tunnel was a suction type, controlled by an inverter. A constant temperature and humidity chamber was used to acquire air temperature and relative humidity required. Nine T-type thermocouples were installed at inlet and outlet of test section respectively, measured air temperatures. The air-side pressure drop across the test section was measured from twelve pressure tapings upstream and downstream respectively, which were connected to a differential pressure transducer with an operating range of 0~25 mmH<sub>2</sub>O gauge. Also to identify the air properties, the

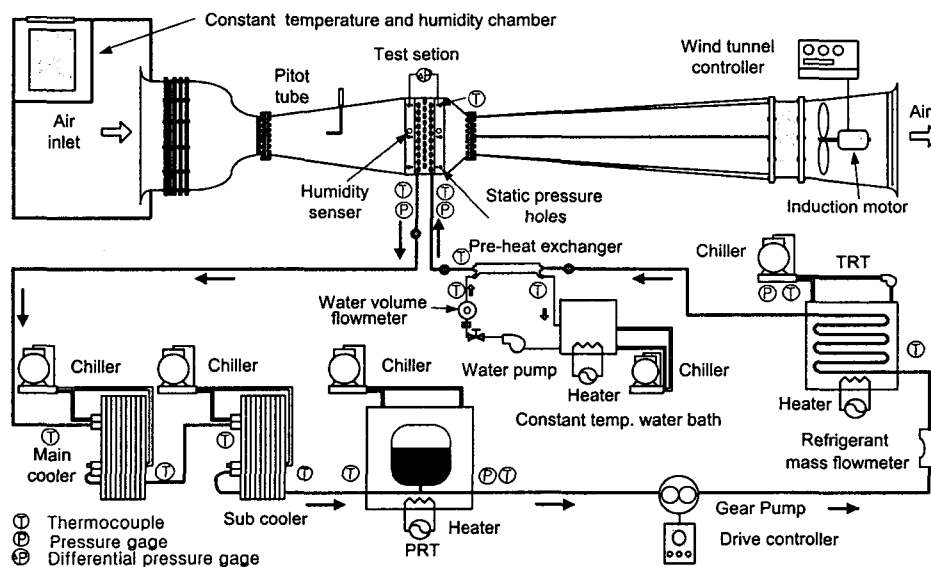


Fig. 1 Schematic diagram of experimental apparatus for condensation test system.

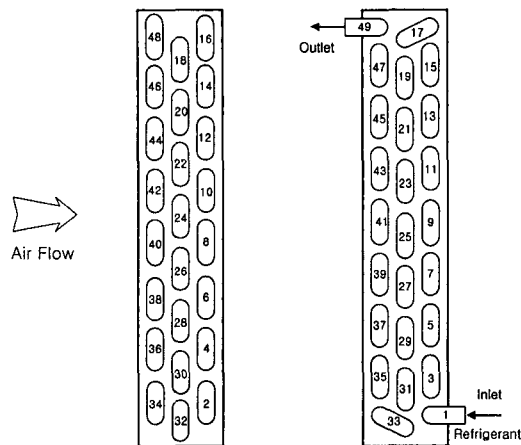


Fig. 2 Locations of measuring temperatures in accordance with flow direction.

relative air humidity was measured at the inlet and at the outlet of test section by humidity transmitter with an uncertainty of  $\pm 2\%$ .

The refrigerant flow loop consists of a variable speed magnetic positive displacement gear pump that delivers subcooled refrigerant to the temperature regulating tank. A compressor requires oil to be dissolved in the refrigerant, however, using a pump eliminates the need for lubrication in the refrigeration system, therefore a pump is used in order to eliminate the effect of lubrication on the condensing process.

The magnetic positive displacement pump is regulated by an inverter. The mass flow rate of the refrigerant is measured using a mass flowmeter. A pressure regulating tank and a temperature regulating tank are utilized to keep the system pressure and temperature constant during testing.

The pre-heat exchanger was employed to control the degree of superheat entering the test heat exchanger.

Total forty nine T-type thermocouples are silver-brazed on the U-band surfaces for measuring the variation of refrigerant temperatures inside tubes.

2.2 Experimental method

A pressure in all part of system was raised to around 3,103 kPa (450 psi) with dry nitrogen gas in order to check leaks. After the leak test, the temperature and the pressure of refrigerant in both a pressure regulating tank and a temperature regulating tank was controlled to the test conditions required. Refrigerant was circulated by means of a magnetic positive displacement pump connected to an inverter. A main cooler and a subcooler were employed to maintain refrigerant passed the test section subcooled. After the temperature and relative humidity of air in the chamber were controlled to the test conditions as presented in Table 2, the wind tunnel was run. Finally the refrigerant liquid was superheated in the preheat exchanger to obtain a 10°C superheat before entering the test section. The primary parameters observed during the experiment were heat transfer rate and pressure drop as a function of refrigerant flow rate and air flow rate at a subcooling temperature of 5°C leaving the test section.

R410A is a azeotropic mixture with a very small temperature glide of 0.1°C (dew tempera-

Table 2 Experimental conditions

Air	Dry bulb temperature	35°C
	Relative humidity	50%
Refrigerant	Refrigerant	R22, R407C, R410A
	Mass flux (kg/m <sup>2</sup> s)	150, 200, 250
	Condensation temperature(°C)	50
	Inlet superheat (°C)	10
	Outlet subcooling temperature (°C)	5

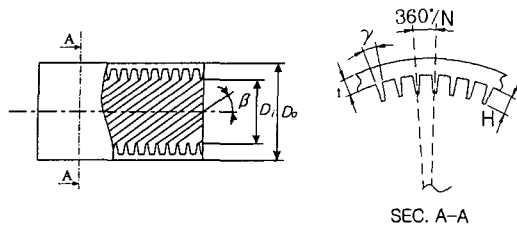


Fig. 3 Characteristic geometrical parameters of micro-fin tube.

ture–bubble temperature) during phase change, whereas R407C has a temperature glide of about 7.2°C at 50°C condensation temperature, so the average of both dew temperature and bubble temperature was employed as a condensation temperature of R407C.

The thermodynamic and thermophysical prop-

Table 3 Geometric dimensions of the heat exchanger tested

Parameter	Specification
Number of tubes per row	16
Number of tube rows	3
Tube outside diameter	9.52 mm
Horizontal tube spacing	21.65 mm
Vertical tube spacing	25 mm
Fin density	493 fins/m
Coil height	400 mm
Air flow length	80 mm
Fin height of tube	0.2 mm
Tube material	Copper
Fin material	Aluminium
Tube rows alignment	Staggered type
Fin type	Slit

Table 4 Geometrical data on the micro-fin tube

Parameter	Specification	
$D_o$	Outer diameter	$9.52 \pm 0.05$ mm
$D_i$	Inner diameter	8.25 mm
$t$	Tube thickness	$0.3 \pm 0.03$ mm
$H$	Fin height	$0.2 \pm 0.02$ mm
$N$	Number of fins	60
$\beta$	Helical angle	$18 \pm 2^\circ$
$\gamma$	Fin angle	$53 \pm 10^\circ$

erties of refrigerant (single and mixtures) have been computed by Refprop version 6.01<sup>(8)</sup> by NIST, and the humidity air properties have been calculated using an equation derived from a psychrometric chart in a ASHRAE handbook.<sup>(9)</sup>

The geometry of heat exchanger used in this study was given in Table 3 and Table 4.

### 2.3 Data reduction and uncertainty

Typical condensation process in a fined-tube heat exchanger may involve superheated single-phase, saturated condensation, and subcooled single-phase heat transfer.

In superheated single-phase heat transfer region, the heat transfer rate from the refrigerant to the air can be calculated from

$$Q_v = m_r(h_{sup} - h_v) \quad (1)$$

In two-phase heat transfer region, the heat transfer rate can be obtained from

$$Q_{tp} = m_r h_{fg} \quad (2)$$

In subcooled heat transfer region, the heat transfer rate from the refrigerant to the air can be calculated from

$$Q_l = m_r(h_l - h_{sub}) \quad (3)$$

Thus the total heat transfer rate in the test section can be described from the following equation.

$$Q_r = Q_v + Q_{tp} + Q_l \quad (4)$$

The heat transfer characteristics are significantly different along the condenser. Generally LMTD or  $\epsilon$ -NTU method are employed to obtain the heat transfer coefficient on a heat exchanger. While heat transfer coefficient was evaluated by means of measuring tube surface temperatures in this study. The temperatures

Table 5 Parameters and estimated uncertainties

Parameter	Uncertainty
Temperature (°C)	±0.75%
Pressure (kPa)	±0.25%
Mass flow rate of refrigerant (kg/s)	±0.20%
Heat transfer rate of refrigerant (kW)	±0.72%
Heat transfer coefficient (kW/m <sup>2</sup> K)	±4.25%

were measured on forty nine locations, namely, forty eight sections, in order to estimate and distinguish the flow region. Even though superheated heat transfer and subcooled heat transfer equivalently have an effect on total heat transfer coefficient, like two-phase heat transfer, for simplicity, only two-phase condensation heat transfer coefficient are evaluated as the following equation. The copper tube used in this experiment has a high thermal conductivity, typically the temperature difference between  $T_{wi}$  and  $T_{wo}$  is less than 0.03 K, it can be assumed that  $T_{wi}$  is approximately equal to  $T_{wo}$ .

$$h_{tp} = \frac{Q_{tp}}{A(T_{sat} - T_w)} \quad (5)$$

$$A = \pi D_{i,m} L \quad (6)$$

where  $T_{sat}$  is the saturation temperature of the refrigerant,  $A$  is the heat transfer area of inside tube,  $D_{i,m}$  is the average inner diameter of tube, and  $L$  represents the tube length that two-phase region occupies.

The uncertainties of the experimental results was analyzed by the procedures proposed by Kline and McClintock.<sup>(10)</sup> The detailed results from the present uncertainty analysis for the experiments conducted here are summarized in Table 5.

### 3. Results and discussion

#### 3.1 Refrigerant temperature distribution

Figure 4 shows the refrigerant temperatures

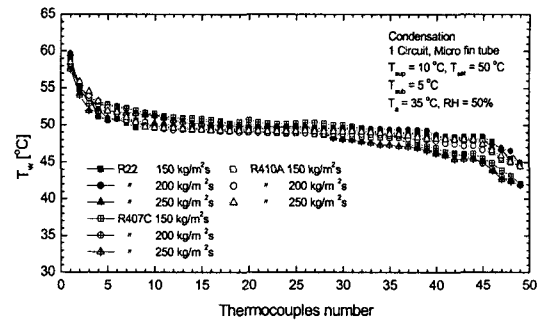


Fig. 4 The variation of tube wall temperatures as a function of refrigerant mass flux.

on U-band surfaces as a function of mass flux at the conditions that the outlet subcooling temperature maintains 5°C. Temperature variation for R407C is relatively bigger than those of R22 and R410A. Superheated region, two-phase region, and subcooled region can be approximately observed and distinguished from the shape of temperature distributions, and there are no significant difference of the among the wall temperature distributions in accordance with mass flux, because the outlet subcooling temperature was continuously kept 5°C.

#### 3.2 Refrigerant pressure drop

Figure 5 shows the behaviors of refrigerant pressure drop for all refrigerants in accordance

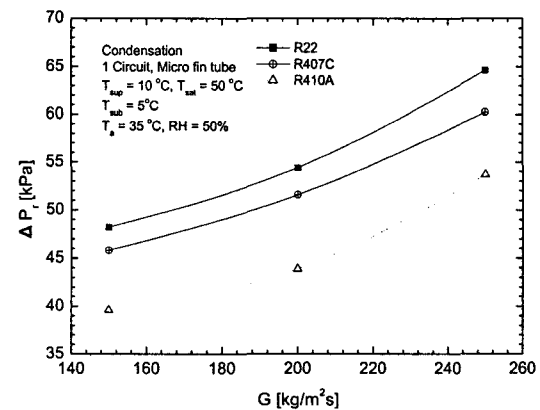


Fig. 5 Pressure drop of refrigerants as a function of mass flux.

with the change of mass flux at the constant outlet subcooling temperature. As expected, as refrigerant mass flux increases, pressure drop increases. For the mass flux range of 150 to 250 kg/m<sup>2</sup>s, the pressure drops for R407C and R410A are 4~12% and 17~26% lower than R22 respectively. The experimental data for Wang et al.<sup>(11)</sup> showed similar results. They reported the flow pattern difference between R22 and R407C might cause this phenomenon.

As condensation process proceeds, the least volatile component of the R407C mixture, R134a condenses faster than the more volatile components of the R407C mixture, R32 and R125. As a result, the liquid phase may contain more R134a as compared to its initial concentration.

From the physical properties for R32, R125, and R134a evaluated at 20°C, we can easily find that the vapor density ( $\rho_v$ ) for R32 is 40.6 kg/m<sup>3</sup>, which is 46.7% higher than that of R134a; and  $\rho_v$  for R125 is 77.8 kg/m<sup>3</sup>, which is 280.7% higher than that of R134a. Meanwhile, the liquid density ( $\rho_l$ ) for R32 is 981.7 kg/m<sup>3</sup>, which is 20% lower than that of R134a; and  $\rho_l$  for R125 is almost the same as that of R134a.

Considering a fixed mass flux condition, the higher mean density of liquid because of the contribution of R134a results in lower mean liquid phase velocity. Therefore, compared to R22, lower mean gas and liquid phase velocities are likely for the mixtures R407C and R410A during the condensation process. As a result, the pressure drops of R407C and R410A are lower than that of R22.

### 3.3 Condensation heat transfer coefficient

Figure 6 shows the variation of two-phase heat transfer coefficients for R22, R407C and R410A versus refrigerant mass flux with a fixed inlet and outlet temperature condition during the condensation process. It is evident from

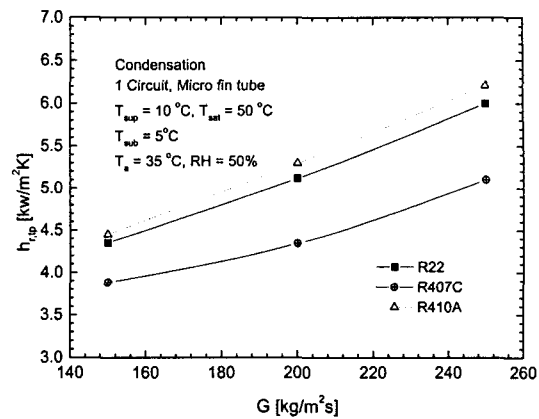


Fig. 6 Condensation heat transfer coefficient as a function of mass flux.

the two phase condensation experimental data displayed in the Fig.6 that R407C has the lowest heat transfer rate compared to the other refrigerants in the investigated range of mass flux, and operating conditions. The heat transfer coefficient of an azeotropic mixture, R410A is 3% higher than that of R22, and the heat transfer coefficient of a zeotropic mixture, R407C is 14% lower than that of R22. The condensation process of zeotropic mixtures is different from pure substance or nearly azeotropic mixture. This is mainly due to the high concentration of R134a in the mixture, which in turn increases the gliding temperature difference of the mixture. This results in decreasing the heat transfer coefficient, and it is in agreement with what has been reported in the literature by Sami and Maltais,<sup>(12)</sup> Cavallini et al.,<sup>(13)</sup> and Hwang<sup>(14)</sup> also it was found that the flow pattern development of R407C falls behind R22 at the same condition by Wang et al.<sup>(11)</sup> by means of flow visualization.

### 3.4 Pressure drop and correlations

Figure 7 shows the comparisons of the experimental pressure drop data which were obtained at the outlet subcooling temperature fixed to 5°C with Eq. (7) from Haraguchi et al.<sup>(15)</sup>

and Eq. (8) from Choi<sup>(16)</sup>

$$\Delta P_{fp} = \frac{2f_v G^2 v_v L}{D_m} \phi_v^2 \quad (7)$$

where  $\phi_v$  represents frictional multiplier,  $f$  is friction factor,  $D_m$  is the average inner diameter of tube.

$$\Delta P_{fp} = \left[ \frac{f_n (v_o + v_i) \Delta L}{D_h} + (v_o - v_i) \right] G^2 \quad (8)$$

where  $f_n (= 0.0185 \text{Re}^{-0.25} K_f^{0.25})$  is a friction factor based on Reynolds number, and  $K_f$  is two-phase number.  $v_o$  is a specific volume at outlet, and  $v_i$  is a specific volume at inlet.

All terms which represent friction, acceleration, and bend pressure drop are included in the calculation of pressure drop. Also each pressure drop occurred in superheated flow region, two phase flow region, and subcooled flow region are contributed to the calculation of total pressure drop. At refrigerant mass fluxes of 200 and 250 kg/m<sup>2</sup>s, the experimental results agreed with the predicted values by the correlations of Haraguchi et al.<sup>(15)</sup> and Choi<sup>(16)</sup> within +30~−10%, at refrigerant mass flux

of 150 kg/m<sup>2</sup>s, the deviation between the experimental and predicted values was more than +30%.

For a higher mass flux range, pressure drop are well predicted by correlations in the contrast to a lower mass flux range. Also generally, correlations used in this study underestimates the experimental pressure drop. The reason probably results from the difference between experimental models used to correlations development and test model used in this study. Also, most existing correlations were developed from experimental studies on a single horizontal tube, not included the consideration of gravitational pressure drop. The pressure drop of an actual finned-tube heat exchanger which is composed of a lot of single horizontal round tubes like this study, obviously contains gravitational pressure drop additionally.

### 3.5 Heat transfer coefficient and correlations

Figures 8~10 present the comparisons between the experimental two phase heat transfer coefficient and those calculated by the proposed correlations.

The correlations proposed by Kedzierski<sup>(17)</sup> and Cavallini<sup>(13)</sup> are derived from the experi-

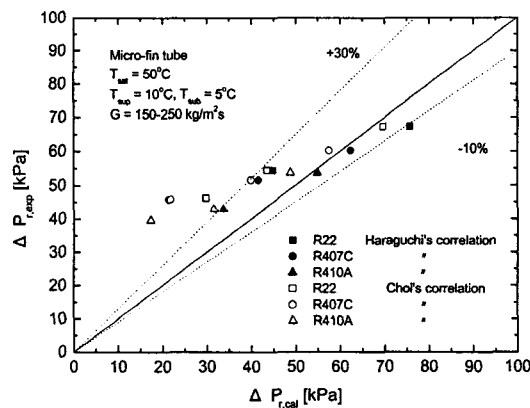


Fig. 7 Comparison of measured refrigerant pressure drop with Haraguchi's and Choi's correlation.

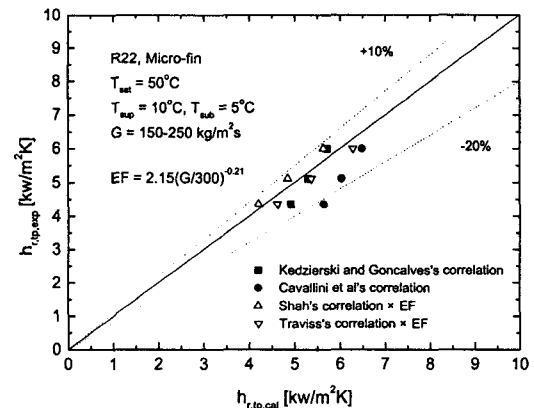


Fig. 8 Comparison of present result with selected correlations for R22.



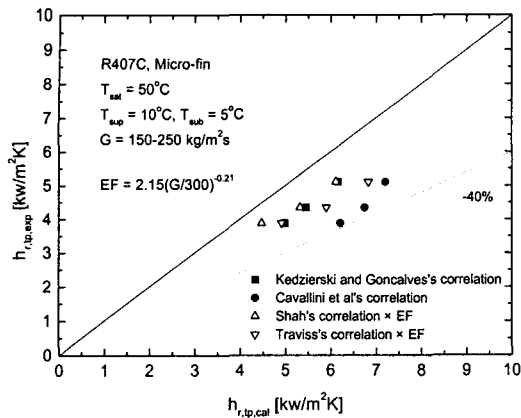


Fig. 9 Comparison of present result with selected correlations for R407C.

mental data on micro-fin tubes and the correlations presented by Shah<sup>(19)</sup> and Traviss<sup>(20)</sup> come from the experimental data on smooth tubes. However, using the modified correlations which are multiplied by enhancement factor, it is possible to estimate the heat transfer coefficient of micro-fin tubes.

Figure 8 shows that the values predicted by all correlations considered in this study agree with the experimental results within +10~−20% for R22. As shown in Fig. 9, experimental two phase heat transfer coefficients for R407C are up to −40% lower than the predicted values.

It is necessary to modify the existing correlations which have been used for estimating the heat transfer coefficient of pure refrigerants in order to predict the heat transfer coefficient of zeotropic refrigerants well. Jung et al.<sup>(21)</sup> also reported the same views as the present opinion.

Figure 10 shows the experimental heat transfer coefficient for R410A compared to the heat transfer coefficient evaluated with the correlations, the deviations between the experimental values and the predicted values are less than R407C.

Kedzierski's correlation estimates the present data in the range of deviations between −10 and +10%, it gives the best agreement with

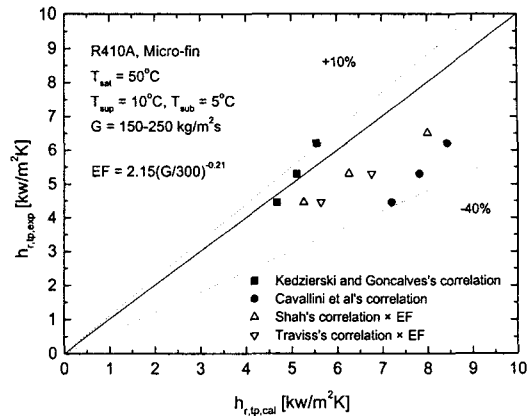


Fig. 10 Comparison of present result with selected correlations for R410A.

the present data.

Other correlations predict the two phase heat transfer coefficient up to −40% higher than experimental values.

The results here indicate that the existing two-phase condensation heat transfer correlations are not appropriate to predict the heat transfer performance of the zeotropic mixture; therefore, further investigations are needed to establish a suitable correlation.

#### 4. Conclusions

An experiment has been carried out in the present study to measure the heat transfer coefficient for the condensation of R22, R410A, and R407C in a slit fin-and-tube heat.

The experiment is conducted under the superheated inlet condition and subcooled outlet condition like an actual operating conditions.

The experimental data have been compared with predictions by several existing correlations, the following conclusions are made:

(1) Condensation heat transfer coefficient of azeotropic refrigerant mixture, R410A is 3% higher than that of R22, and average pressure drop is 20% lower than that of R22.

Also, average air velocity is required 16% less than R22 in order to obtain the same con-

condensation performance, so, it results in power saving, noise reduction, and compactness of equipment. Therefore, R410A is considered as the strongest candidate among alternative refrigerant mixtures for R22, rather than R407C.

(2) When the values of condensation heat transfer coefficients calculated by the selected correlations have been compared with the experimental ones, the experimental data for R22 are in the best agreement with the selected correlations, but those for R407 show the worst agreement. The condensation heat transfer coefficient correlation proposed by Kedzierski shows the best agreement with the experimental data.

### References

1. Molina, M. J. and Rowland, F. S., 1974, Stratosphere sink for chlorofluoromethanes; Chlorine atom catalyzed destruction of ozone, *Nature*, Vol. 249, pp. 810-812.
2. Kim, M. H., Shin, J. S. and Kim, K. J., 1997, An experimental study on the performance of a window system air-conditioner using R407C and R410B, *Korean Journal of Air-Conditioning and Refrigerating Engineering*, Vol. 9, No. 4, pp. 536-544.
3. Ebisu, T. and Torikoshi, K., 1995, Experimental studies on cross-flow heat exchanger performance using non-azeotropic refrigerant mixture, *Proceedings of 19th International Congress of Refrigeration*, 4a, pp. 163-170.
4. Ebisu, T., Kasai, D. and Torikoshi, K., 1996, A study thermal performance of air-cooled heat exchangers using alternative refrigerant, *33rd National Heat Transfer Symposium of Japan, Nigata*, Vol. 2, pp. 525-526.
5. Chen, S., Judge, J. F., Groll, R. and Radermacher, R., 1994, Theoretical analysis of hydrocarbon refrigerant mixtures as a replacement for R-22 for residential uses, *Proceedings of 1994 International Refrigeration Conference at Purdue University, West Lafayette, Indiana, USA*, pp. 225-230.
6. ARI, Participants Handbook: R-22 Alternative Refrigerants Evaluation Program (AREP), June 1993, ARI.
7. Ryuzaburo, Y., Nobumo, D., Sigeharu, T., Isamu, T., Ebisu, T. and Torikoshi, K., 1994, In-tube heat transfer characteristics of refrigerant mixtures of HFC-32/134a and HFC-32/125/134a, *Proceedings of 1994 International Refrigeration Conference at Purdue*, pp. 293-298.
8. McLinden, M. O., Klein, S. A., Lemmon, E. W. and Peskin, A. P., 1998, Thermodynamic and transport properties of refrigerants and refrigerant mixtures database (REFPROP), Ver. 6.01, NIST.
9. ASHRAE, 1993, *Fundamental Handbook (SI)*.
10. Kline, S. J. and McClintock, F. A., 1953, Describing uncertainties in single sample experiments, *Mechanical Engineering*, Vol. 75, pp. 3-8.
11. Wang, C. C. and Chiang, C. S., 1997, Two-phase heat transfer characteristics for R22/R407C in a 6.5 mm smooth tube, *Int. J. Heat and Fluid Flow* 18, pp. 550-558.
12. Sami, S. M. and Maltais, H., 2000, Experimental investigation of two phase flow condensation of alternatives to HCFC-22 inside enhanced surface tubing, *Applied Thermal Engineering*, Vol. 20, pp. 1113-1126.
13. Cavallini, A., Censi, G., Col, D. Del, Doretto, L., Longo, G. A. and Rossetto, L., 2001, Experimental investigation on condensation heat transfer and pressure drop of new HFC refrigerants, *International Journal of Refrigeration*, Vol. 24, pp. 73-87.
14. Hwang, S. M., 1999, Condensation heat transfer coefficients of R22 alternative refrigerants on enhanced tubes, *International Journal of KSME*, Vol. 23, No. 4, pp. 459-469.
15. Haraguchi, H., Koyama, S., Esaki, J. and Fujii, T., 1993, Condensation heat transfer of refrigerants HFC134a, HCFC123 and HCFC22 in horizontal smooth tube and a

- horizontal micro fin tube, Proc., 30th National Symposia of Japan, Yokohama, pp. 343-345.
16. Choi, J. Y., 1999, Study on the prediction of pressure drop for condensation and evaporation of alternative refrigerants in micro-fin tubes, Yonsei University, Seoul, Korea.
  17. Kedzierski, M. A. and Goncaves, J. M., 1997, Horizontal convective condensation of alternative refrigerant within a micro-fin tube, NISTIR 6095, US Dept. Commerce.
  18. Cavallini, A., Doretti, L., Klammsteiner, N., Longo, G. A. and Rossetto, L., 1995, Condensation of new refrigerant inside smooth and enhanced tube, Proceeding 19th International Refrigeration Conference at Hague, Vol. 4, pp. 105-114.
  19. Shah, M. M., 1979, A general correlation for heat transfer during film condensation inside pipes, Journal of Heat and Mass Transfer, Vol. 22, pp. 547-556.
  20. Traviss, D. P., Rohsenow, W. M. and Baron, A. B., 1972, Force convection condensation inside tube: a heat transfer equation for condenser design, ASHRAE Transactions, Vol. 79, pp. 157-165.
  21. Jung, D. S., Bae, J. S., Lee, Y. H., Song, Y. J. and Lee, J. K., 1998, Predict pool boiling heat transfer coefficients of pure and mixed refrigerants, Report of Inha University.